

Tu STZ2 05

Using Geophysical Well Logs to Estimate the Porosity System of Albian Carbonates of Campos Basin - Rio de Janeiro

C. de Abreu* (UENF) & A.A. Carrasquilla (North Fluminense State University (UENF))

SUMMARY

Albian carbonates are important oil reservoirs on the NE coast of Rio de Janeiro. In this work, aiming to evaluate the porosity of these deposits, we used basic well logs, geological information and petrophysical laboratory data from two oil fields of this region. However, proposed models to study this kind of reservoirs consider combinations of porosities derived from density and neutron logs, but do not recognize the importance of sonic porosity in the identification of fractures that distort the porosity models when they are compared with experimental data. Still, joint analysis of porosities derived from these three logs is addressed in this study and a new regression is proposed, which showed high correlation with the petrophysical data in both fields, regardless the differences of diagenetic processes that every oil field was submitted. Furthermore, the linear regression model applied to the calculation of Archie's cementation coefficient (m) demonstrated that in zones with not connected porosity the value of m will be greatly increased and should not to be considered to calculate the saturation. Finally, using porosity cross plots derived from density and sonic logs allowed to identify different kind of porosities and to visualize the effective porosity along the geological formations.

Introduction

The central idea of this work is to generate post-salt carbonate reservoirs models to thereby contribute to the knowledge of the carbonate reservoirs of the Brazilian pre-salt layer. At work, carbonate reservoirs of Quissama Formation in Campos Basin on the northeast coast of Rio de Janeiro were studied, which belong to the Cretaceous, Albian of age, with a nature marine sedimentation and transgressive depositional environment of shallow platform. According Guardado *et al* (1990, this formation consists of carbonate banks dominated by grainstones and packstones stacked on sea level change cycles and composed of ooids, oncoids, peloids and bioclasts. The study proposed to evaluate the porous system of these reservoirs through the integration of petrophysical data laboratory, geological and well log data and thus generate results that contribute to the exploration and production oil. It was used Interactive Petrophysics (IP, 2015) software for interpretation of geophysical logs, in order to compare these interpretations, especially porosity, with the core samples petrophysical properties measures in laboratory.

Methodology

The studied oil fields were named A and B, where two wells of each were provided (A3, A10 and B17, B29) with their respective datasets, consisting in the basic suite of logs (GR, RES, NPHI, RHOB and DT), geological information and petrophysical laboratory measurements. The porosity was initially estimated using NPHI, RHOB and DT logs individually and then compared to the porosity estimated in the laboratory for the Field A. Another initiative used in this study was to evaluate the applicability of previously published equations to calculate the porosity. In the second step, Field B was evaluated, noting that a joint analysis of estimated porosities provides a perspective to clean the distortions between them, allowing you to build a categorization. In the tertiary phase of work was utilized a multiple linear regression applied to estimate the porosity in both fields, based along the individual porosities estimated. As the cementing relates to porosity, the Archie's cement factor m was calculated for the well that showed the best applicability of overlapping analysis of porosity and, finally, it was possible to sort the porosity through of sonic and density porosity crossplots.

Results

Initially, the porosities were calculated to well A3 using the RHOB (PHID), NPHI (PHIN) and DT (PHIS) logs, which appear in Figure 1 together with laboratory measured porosity (PHILAB). PHIS fits best the PHILAB values in X793, X802, X838, X840 and X852 depths, as well as PHID shows a reasonable fit and PHIN the worst performance. Then, we apply the Raymer *et al.* (1980), Doveton (2014), Dubois *et al.* (2006) and Crain (1986) proposals to estimate the porosity. The Raymer's approach considers P wave velocity, but the other only combinations of PHID and PHIN. In Figure 2, in tracks 3, 4, 5 and 6, these porosities are plotted together with PHILAB with any of them showing a good fit. Whereas PHIS was the one that generated the best fit for this well, it was to be expected that these proposals did not give a good performance. So, in search of a better estimate, we used a multiple linear regression (MLR), generating the equation $PHIMLR = 3.5 + 23.2 (PHID) - 0.14 (PHIN) + 63.2 (PHIS)$, which shows a higher weight to PHIS. In Figure 3 are plotted the PHID, PHIN, PHIS, PHILAB and PHIMLR porosities, the latter giving a better fit with a Pearson correlation coefficient (R2) of 0.33, being even better than PHIS in X807, X827, X836 depths.

The determination of the value of m was taken by the Archie Equation (1942) and by Shell formula (Schon, 2011). Figure 4 shows the curve generated for m in well B17 and, as claimed Lucia *et al.* (1983) and Ahr (2011), in the presence of not connected porosity, m can reach values of 3 to 4 and in fractured zones close to 1. In the figure, we can see that in the region with not connected porosity m is around 2 and in the fracture zones in the order of 1.5. So, considering very high or very small m values can make a large error in the calculation of saturation. On the other hand, the PHIS vs PHID cross plot for this well is shown in Figure 5, where the intergranular porosity predicted by equation Wyllie (Wyllie *et al.*, 1956) remains on the line of 45° and the deviations show the occurrence of possible fractured or cracking, micro - porosity and not connected porosity regions (Brie *et al.*, 1985), which

appear differentiated by color scale. Finally, Figure 6, in the third track, shows the PHID, PHIN, PHIS, PHIMLR and PHILAB porosities plotted together, with PHIMLR presenting a better fit. In this figure, through colorful horizontal lines, we can identify in blue not connected porosities, in red zones with fractures or cracking, in orange microporosity and in pink intergranular porosity. In X360 it can be identify a micro - porosity connected region, as PHIS shows higher values than PHID, i.e., the connected porosity is greater than the true porosity, being that, in this case, PHID is the porosity to be considered with PHIS showing only that the micro - porosity is connected. Between X370 to X440 will have a very fractured region that impact the effective porosity. From X445 to X500 we identify the presence of not connected porosity zones, which should be disregarded from the computation. The intergranular porosity is identified throughout the well.

Conclusions

In this work, the selection of two fields with different petrophysical characteristics, although both are Albian carbonates and belong to Quissama Formation, it was very important to study their porosities. By examining the conflicts between the logs was possible to identify the relevance of DT log to determine the effective porosity, as considerably as the importance of joint analysis of DT, NPHI and RHOB logs to calculate the porosity. The linear regression models presented, which take into considering the PHIS, PHIN and PHID porosities, demonstrated a high correlation with petrophysical data in both fields, regardless of diagenetic differences that each field has been submitted. The linear regression model applied to the calculation of cementing coefficient (m) demonstrated that in areas with not connected porosity the value of m will be greatly increased and cannot to be considered for the calculation of saturation in these regions. It was demonstrated even in the fractured regions the value of m will be close to 1. The use of PHIS - PHID porosities cross plot allowed a qualitative analysis and identification of different porosities present, while still allowing the visualization of the effective porosity along the borehole.

References

- Ahr, W. [2011] *Geology of carbonate reservoirs: the identification, description and characterization of hydrocarbon reservoirs in carbonate rocks*. John Wiley & Sons.
- Archie, G. [1942] The electrical resistivity log as an aid in determining some reservoir characteristics. *I. Pet Tech*, **5**.
- Brie, A., Johnson, D. and Nurmi, R. [1945] Effect of spherical pores on sonic and resistivity measurements. *26th Annual Logging Symposium*. SPWLA, **1**.
- Crain, E. [1986] *Log analysis handbook*. PennWell Books, Tulsa, OK.
- Doveton, J. [2014] *Principles of Mathematical Petrophysics*. Oxford University Press.
- Dubois, M., Byrnes, A., Bohling, G. and Doveton, J. [2006] *Multiscale geologic and petrophysical modeling of the giant hugoton gas field (permian), Kansas and Oklahoma, USA*. AAPG Special Volumes.
- Guardado, L., Gamboa, L. and Lucchesi, C. [1990] Petroleum geology of the Campos Basin, Brazil, a model for a producing Atlantic type basin. Divergent/passive margin basins. *AAPG Memoir*, **48**, 3-79.
- Lucia, F. *et al.* [1983] Petrophysical parameters estimated from visual descriptions of carbonate rocks: a field classification of carbonate pore space. *JPT*, **35**(3), 629-637.
- IP. [2015] *Interactive Petrophysics Users' Manual*.
- Raymer, L., Hunt, E. and Gardner, J. [1980] An improved sonic transit time-toporosity transform. In: *Trans. SPWLA 21st Annu. Log. Symp.*, P1-P13.
- Schön, J. [2011] *Physical properties of rocks: A workbook*. [S.l.]: Elsevier.
- Wyllie, M., Gregory, A. and Gardner, L. [1956] Elastic wave velocities in heterogeneous and porous media. *Geophysics*, **21**(1), 41-70.

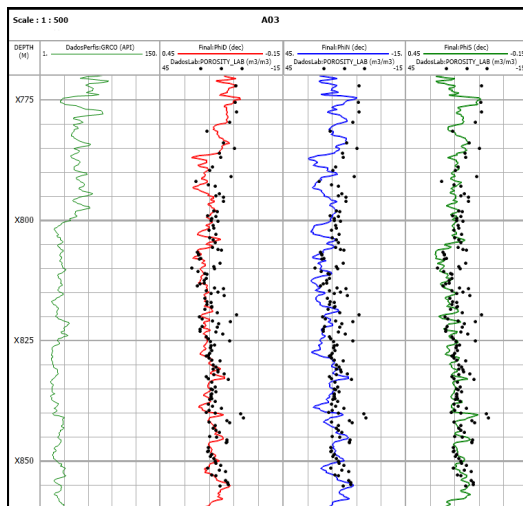


Figure 1 Porosity estimates for well A3 using RHOB (track 2), NPHI (track 3) and DT (track 4) logs plotted together with the PHILAB porosity (dark dots).

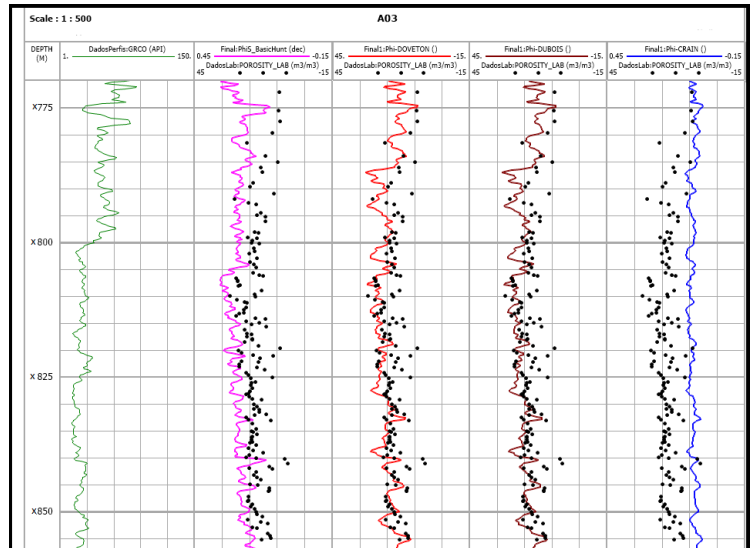


Figure 2 Porosity estimates for well A3 using the equations proposed by Raymer-Hunt-Gardner (track 2); Doveton (track 3); Dubois (track 4) and Crain (track 5) plotted together with the PHILAB porosity (dark dots).

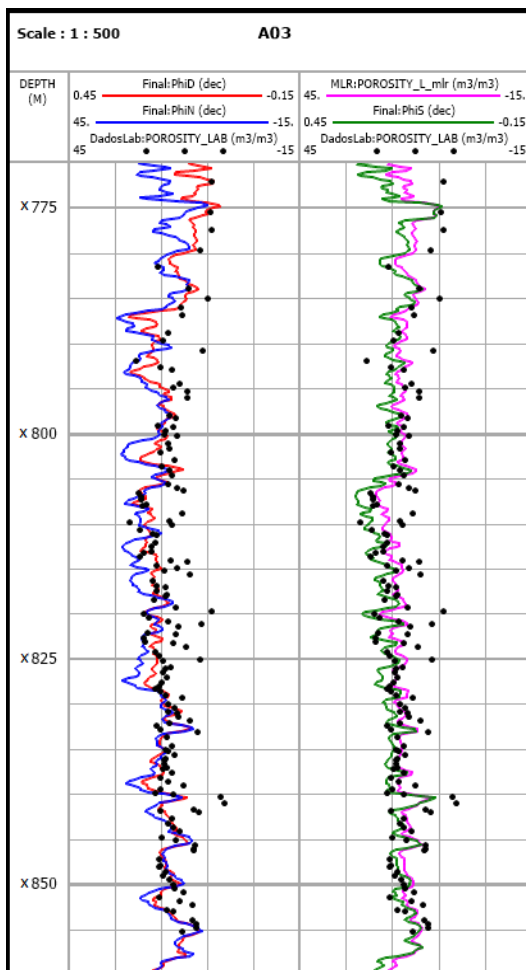


Figure 3 Porosity estimate using a multiple linear regression for well A3 plotted together with the PHID and PHIN (track 2), PHIS and PHILMR (track 3) plotted together with PHILAB porosities (dark dots).

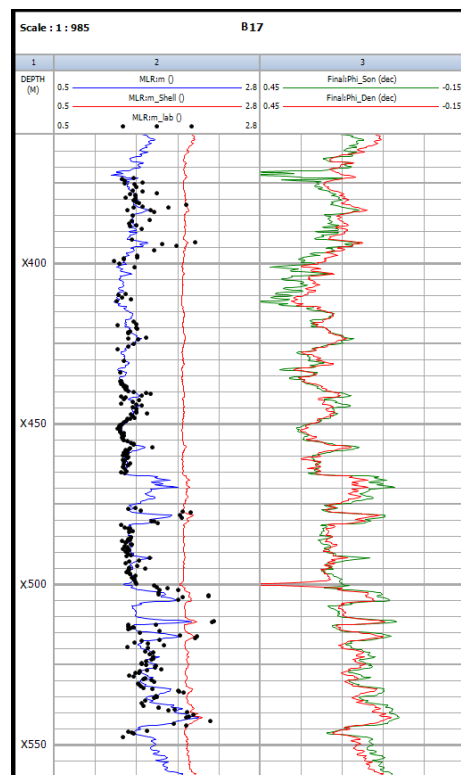


Figure 4 Estimates of m for well B17 (track 2): Archie's equation (dark dots), Shell formula (red curve) and linear regression (blue curve).

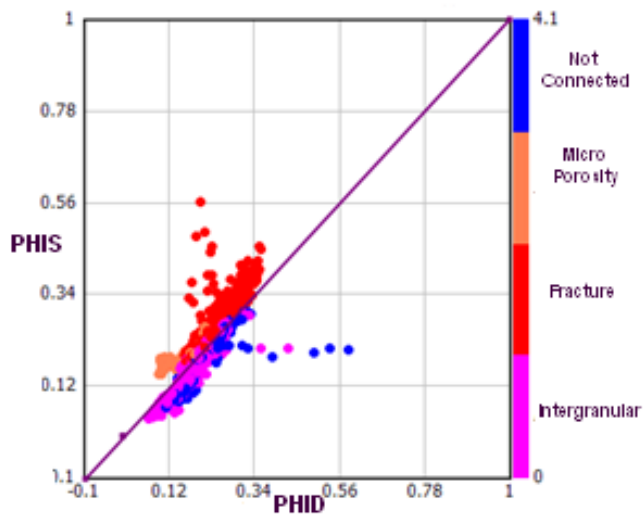


Figure 5 Porosity classification for well B17 using PHID vs PHIS cross plot.

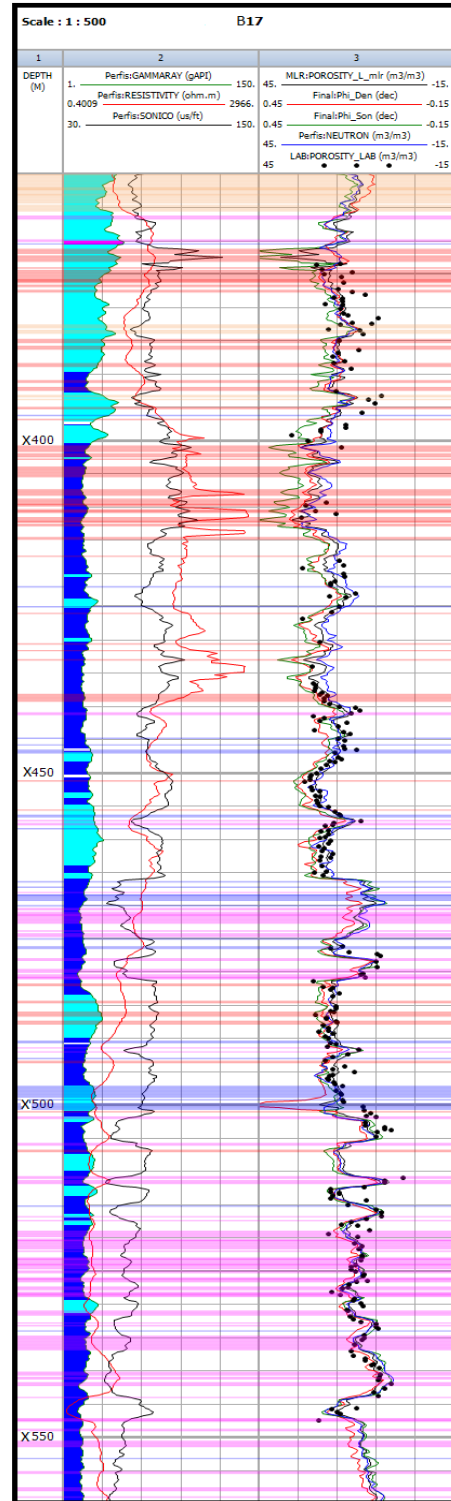


Figure 6 Porosity rating (colored lines) over the well B17 based on the cross plot of Figure 5.